Journal of Chemical Engineering of Japan, Vol. 48, No. 7, pp. 556–563, 2015 **Research Paper**

Solid–Liquid Separation Properties in Centrifugal Sedimentation of Bidisperse Colloidal Suspension

Da-Qi Cao, Eiji Iritani and Nobuyuki Katagiri

Department of Chemical Engineering, Nagoya University, Furo-cho, Chikusa-ku, Nagoya-shi, Aichi 464-8603, Japan

Keywords: Centrifugation, Sedimentation, Bidisperse Suspension, Porosity, Sedimentation Coefficient

The present study investigates solid–liquid separation behaviors in centrifugal sedimentation for concentrated bidisperse colloidal suspensions containing polymethylmethacrylate (PMMA) particles of two different submicron sizes with equal densities, using an analytical centrifuge. The sedimentation coefficient for describing the settling rate of the interface separating the dispersion from clear liquid was determined from the sedimentation curve drawn based on the measurements of near-infrared light transmission. It was found that the sedimentation coefficient decreased with decreasing porosity and increasing ratio of the volume of small particles to volume of total particles, while it was little influenced by the initial height of suspension and the angular velocity of the rotor. A model was developed for describing the relation between the sedimentation coefficient and porosity in a suspension in the centrifugal sedimentation of a bidisperse suspension. In the low concentration region, the sedimentation coefficient was determined from the settling rate of small particles because small particles settled independently from large particles in the upper zone. In contrast, the sedimentation coefficient in the high concentration region was obtained based on the mean specific surface area size of small and large particles determined using the mixing ratio, since small and large particles settled collectively. In addition, the critical porosity determining the boundary between low and high concentration regions was well described by the model developed. The validity of the model was confirmed by comparing the calculations with experimental data.

Introduction

Sedimentation is one of the typical solid–liquid separation processes and is widely prevalent in industry because of its ease-of-use. The sedimentation behaviors of concentrated bidisperse suspensions serve as the basis for understanding complicated behaviors in the sedimentation of polydisperse suspensions, which are encountered frequently in practice in industrial processes, and hence they have so far been investigated extensively by many researchers, in order to experimentally elucidate the dependence of gravitational sedimentation behaviors on the particle diameter ratio (Krishnamoorthy *et al.*, 2007), particle density ratio (Richardson and Meikle, 1961), segregation (or particle concentration) (Davies, 1968; Hoyos *et al.*, 1994; Cheung *et al.*, 1996), and electrostatic interaction (Iritani *et al.*, 1997). As industrial products have become progressively finer, attention has recently turned to centrifugal sedimentation, which can produce a larger driving force.

A number of studies have been reported over the years on the analysis of the gravity sedimentation of bidisperse suspension (Smith, 1965; Dorrell and Hogg, 2010) or polydisperse suspension (Selim *et al.*, 1983; Ha and Liu, 2002), which was able to be easily extended to the analysis of centrifugal sedimentation of bidisperse suspensions. Although a variety of models (Smith, 1997; Kondrat'ev and Naumova, 2006; Krishnamoorthy, 2010) have been proposed, Lockett and Al-Habbooby (1973, 1974) initially applied the Richardson and Zaki (1954) correlation for monodisperse suspension to bidisperse suspensions, and their model played an important role contributing to the subsequent studies. In the model, equations were presented for separately evaluating the settling velocities of small and large particles by considering the void functions of both particles. However, as the particle concentration increases, it is expected that both small and large particles settle collectively. To achieve a better agreement between the data and predictions Mirza and Richardson (1979) modified the Lockett and Al-Habbooby (1973) model by introducing a purely empirical correction factor.

Recently, an introduced analytical photocentrifuge allowing for the study of the movement of the phase boundary in centrifugation has been used as a powerful tool to analyze the mechanism of centrifugal separation (Lerche, 2002; Detloff *et al.*, 2006; Iritani *et al.*, 2007; Loginov *et al.*, 2012; Cao *et al.*, 2014). The device could be efficiently employed to survey separation behaviors of bidisperse suspensions containing submicron particles.

In the present work, the solid–liquid separation properties in the centrifugal sedimentation of a concentrated colloidal suspension of two-sized spherical particles are investigated using an analytical photocentrifuge. The dependence of the sedimentation coefficient on solids volume fraction (or porosity) in suspensions is examined with varying the ratio of the volume of small to the volume of total particles,

Received on July 11, 2014; accepted on September 6, 2014
DOI: 10.1252/jcej.14we219
Correspondence concerning this article should be addressed to E. Iritani (E-mail address: iritani@nuce.nagoya-u.ac.jp).

initial height of suspension, and angular velocity of the rotor. A model is developed for readily evaluating the settling velocity of the interface between the dispersion and clear liquid on the basis of the concept of critical porosity. The applicability of the model is tested through experimentation.

1. Model Development

In centrifugal settling, the sedimentation coefficient S is defined by

$$S = v/(r\Omega^2) \tag{1}$$

where v is the centrifugal settling velocity, r is the radial distance of an arbitrary position from the center of rotation, and Ω is the angular velocity of the rotor, and thus $r\Omega^2$ indicates the centrifugal acceleration. For a concentrated suspension containing spheres of uniform size and density, S in the above equation is empirically represented by (Richardson and Zaki, 1954)

$$S = S_0\varepsilon^n \tag{2}$$

where ε is the porosity (or voidage) defined as the volume fraction of the continuous phase, and the exponent n is the empirical coefficient ranging from 4.65 to 6.55 in the Stokes region (Heitkam *et al.*, 2013). When the flow is within the Stokes region, S_0 appeared in Eq. (2) is described by

$$S_0 = Cd^2 \tag{3}$$

where d is the Stokes diameter of particles, and C is a constant defined by

$$C = (\rho_p - \rho)/(18\mu) \tag{4}$$

where ρ_p and ρ are the densities of particles and solvent, respectively, and μ is the viscosity of the solvent.

For a bidisperse suspension involving two particle species of different size, but of equal density, the settling behaviors of the interface between dispersion and clear liquid are considered from the viewpoint of solid–liquid separation. It is presumed that sedimentation behaviors of bidisperse suspension are broadly classified into two categories, as shown in **Figure 1**: one is the case where only small particles are settling independently from large particles in an upper sedimenting zone (Figure 1(a)), and the other is the case where small and large particles are settling collectively at the same velocity (Figure 1(b)).

The case shown in Figure 1(a) is normally seen in the sedimentation of a dilute suspension. When settling of large particles has little influence on the settling rate of the interface between the dispersion and clear liquid, the sedimentation coefficient S corresponding to the settling rate can be approximated by

$$S = Cd_S^2\varepsilon_S^n; \quad \varepsilon > \varepsilon_c \tag{5}$$

where ε_c is the critical porosity, which is described in detail later, d_S is the Stokes diameter of small particles, and ε_S is the porosity on a small particle basis calculated from

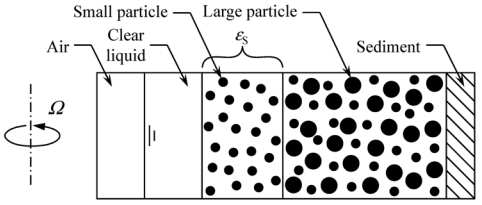

(a) Case where small particles settle independently from large particles

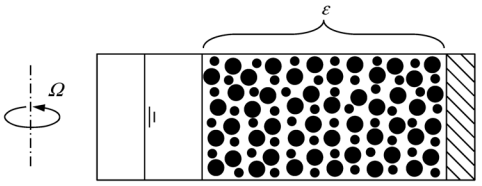

(b) Case where small and large particles settle collectively

Fig. 1 Two types of centrifugal sedimentation behaviors of bidisperse suspension

$$\varepsilon_S = 1 - \alpha_S\phi = 1 - \alpha_S(1-\varepsilon) \tag{6}$$

where α_S is the ratio of the volume of small to volume of total particles, and ϕ is the volume fraction of the total particles.

As the solid concentration in suspension increases, the interaction between small and large particles becomes marked (Davies, 1968) and both particles appear to settle collectively at the same velocity. When the mean specific surface area size d_{av} of small and large particles is employed as a representative diameter describing the sedimentation behaviors in a bidisperse suspension, the sedimentation coefficient S may be written as

$$S = Cd_{av}^2\varepsilon^n; \quad \varepsilon \le \varepsilon_c \tag{7}$$

The diameter d_{av} is defined by

$$d_{av} = \frac{1}{\alpha_S/d_S + (1-\alpha_S)/d_L} \tag{8}$$

where d_L is the Stokes diameter of large particles.

The relation between S and ε is schematically shown in **Figure 2**. The solid and dotted lines are the calculations obtained from Eqs. (5) and (7), respectively. There exists an intersection between two lines where the abscissa is named as the critical porosity ε_c. The sedimentation coefficient S calculated from Eq. (5) is smaller than that calculated from Eq. (7) at porosities larger than ε_c. In contrast, at porosities smaller than ε_c, S obtained from Eq. (7) is smaller than that obtained from Eq. (5). Our model presumes that a smaller S-value in both calculations determines the settling velocity of the interface between the dispersion and clear liquid in the sedimentation of a bidisperse suspension, and this is verified by experimentation, as mentioned later.

As a result, the values of S of a bidisperse suspension may be calculated from the piecewise function of Eqs. (5) and (7). The critical porosity ε_c appearing in Eqs. (5) and (7) can be derived from Eqs. (5) through (8) and represented by

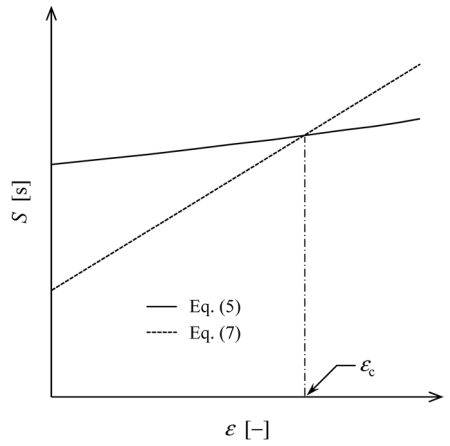

Fig. 2 Schematic view describing relation between sedimentation coefficient and porosity of suspension based on model developed in centrifugal sedimentation of bidisperse suspension

$$\varepsilon_c = \frac{1-\alpha_S}{\{\alpha_S + (1-\alpha_S)d_S / d_L\}^{-2/n} - \alpha_S} \tag{9}$$

As the solid concentration in a suspension increases above the critical value, the interaction between small and large particles becomes very strongly marked (Davies, 1968) and thus all of the particles fall in a group at the same velocity (Coulson *et al.*, 1978). This phenomenon is defined as collective sedimentation (Yoshioka, 1962). Our model is characterized by employing the mean specific surface area size d_{av} of small and large particles as the particle size appearing in the Richardson and Zaki type equation on collective sedimentation of a bidisperse suspension. In contrast to our model, the settling velocities of small and large particles are evaluated separately in the Lockett and Al-Habbooby (1973, 1974) model.

2. Experimental

2.1 Materials and dispersion preparation

The colloidal particles used as the dispersed phase were monodisperse, spherical polymethylmethacrylate (PMMA) (MP-1000, and MP-1600, Soken Chemical & Engineering Co., Ltd.). The hydrodynamic diameters of MP-1000 and MP-1600 particles designated as d_S and d_L were 0.44 and 0.77 μm, respectively, which were determined from the measured Stokes velocities, as mentioned later. The densities ρ_p of both particles were 1,210 kg/m^3, which were measured by means of a pycnometer (Sansyo Co., Ltd.). Ultrapure, de-ionized water ($\rho = 997$ kg/m^3) was produced by purifying tap water through an ultrapure water system equipped with Elix-UV20 and Milli-Q Advantage (Millipore Corp.). The particles were gradually added into ultrapure, deionized water with continuous stirring and well dispersed through sonication for 30 min. As a result, colloidal suspensions with the volume fraction ϕ of 0.35 were provided at various mixing ratios α_S as preparative suspension. The colloidal suspensions with ϕ less than 0.35 were prepared by diluting the preparative suspension with ultrapure, deionized water and used as test samples after the agitation at a stirring rate of 250 rpm for 10 min.

2.2 Experimental apparatus and procedure

Centrifugal sedimentation experiments were carried out at different constant rotor speeds ranging from 1,000 to 3,000 rpm (the angular velocities of the rotor ranged from 104.7 to 314.2 rad/s) corresponding to a centrifugal acceleration of 122–1,098×g with reference to the base of the cell, using a microprocessor-controlled analytical photocentrifuge (LUMiFuge 116, L.U.M. GmbH) (Lerche, 2002; Detloff *et al.*, 2006; Iritani *et al.*, 2007; Cao *et al.*, 2014), where g is the gravitational acceleration. Precision spectroscopic rectangular glass cells with the section of 10 mm length and 1 mm width equal to the optical path length were used. The effect of the cell wall on particle settling was negligible due to the incredibly small ratio (less than 7.7×10^{-4}) of the particle size to the size of the cell section (Francis, 1933). The initial height of the dispersion filled in the cell was varied from 9.99 to 15.67 mm, and the radial distance R from the center of rotation to the bottom of the sample filled in the cell was 108.51 mm. The cells charged with the sample were positioned in the radial direction on the rotor. The instrument non-invasively traced the local and temporal variations of the intensity of transmitted near-infrared (NIR) light at 880 nm over the total length of the sample cell containing the dispersion while centrifugation was in progress. Particle migration due to the centrifugal force causes a variation in the local particle concentration, and correspondingly, the local and temporal variations of the transmission. The transmission profile of the sample during the course of centrifugal sedimentation was continuously recorded by a CCD-line sensor, displayed as a temporal sequence on the computer screen, and saved in a PC. The data was used to determine the time course of the position of the interface of the dispersion and clear liquid, as described in the next section.

3. Results and Discussion

3.1 Determination of sedimentation coefficients

Figure 3 illustrates the typical change with time in the NIR light transmission T expressed in percentage over the entire sample height at the angular velocity Ω of 314.2 rad/s for centrifugal sedimentation of a PMMA bidisperse suspension, where the suspension concentration ϕ is 0.05 and the mixing ratio α_S is 0.75. In this figure, r is the radial distance of an arbitrary position from the center of rotation, and r_0 is the radial distance from the center of rotation to the top of the sample filled in the cell. The transmission profiles were taken every 40 s. The figure implies that only one explicit interface was observed between the dispersion and clear liquid in the concentration range examined in this study, although two interfaces corresponding to the small and large particles, respectively, can be detected by the analytical centrifuge at extremely low concentrations (Detloff *et al.*, 2006). Accordingly, the sedimentation coefficient S

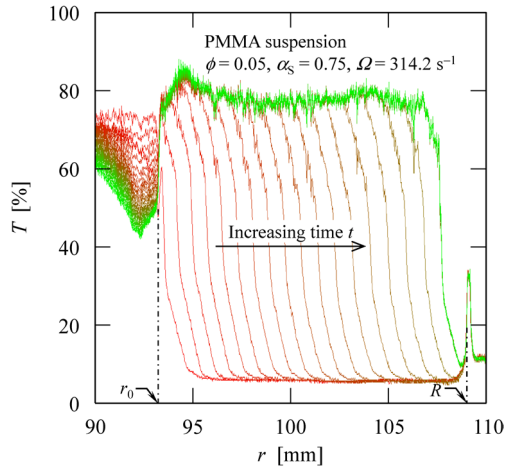

Fig. 3 Typical change with time in NIR light transmission in centrifugal sedimentation of bidisperse suspension

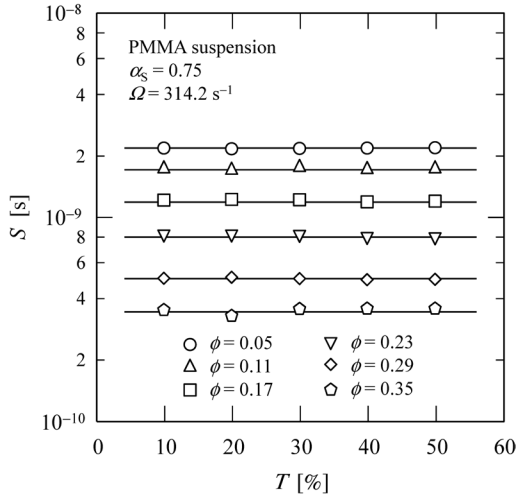

Fig. 4 Effect of NIR light transmission used to determine position of solid–liquid interface on sedimentation coefficient

representing the settling velocity for a unit centrifugal acceleration was determined based on the semi-log plots of the sedimentation interface r_i vs. centrifugal time t using the relation (Moore, 1972; Iritani *et al.*, 1993):

$$S = \frac{1}{r_i \Omega^2} \cdot \frac{dr_i}{dt} = \frac{1}{\Omega^2} \cdot \frac{d(\ln r_i)}{dt} \tag{10}$$

where r_i is the radial distance from the center of rotation to the interface of dispersion and clear liquid.

It is necessary to determine the settling rate of the solid–liquid interface from the temporal variation of the transmission T in order to obtain the sedimentation coefficient S. As an example, the sedimentation coefficient S calculated from Eq. (10) was plotted against the transmission T measured using suspensions with varying ϕ at α_S of 0.75 and Ω of 314.2 rad/s, as depicted in **Figure 4**. While it is difficult to judge the position of the solid−liquid interface accurately from the value of T, it should be noted that the sedimentation coefficient S determined from various T-values remains constant at a given volume fraction. In this study, T of 40%

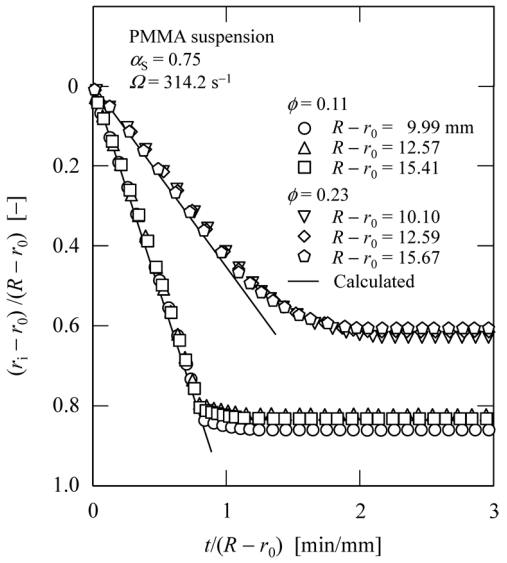

Fig. 5 Effect of initial height of sample on sedimentation rate evaluated as form of normalized sedimentation curve

was adopted in the determination of time variation of r_i in Eq. (10) for all of the experimental data.

3.2 Normalized form of sedimentation curve

In **Figure 5**, the data are plotted in the normalized form of $(r_i - r_0)/(R - r_0)$ vs. $t/(R - r_0)$ for the conditions of $\alpha_S = 0.75$, and $\phi = 0.11$ and 0.23, in order to investigate the effect of the initial height of the sample on the settling velocity. It is found that the plot shows a linear relationship in the initial stage of centrifugal sedimentation, indicating that the sedimentation velocity is maintained almost constant during that stage, since the change of r_i during sedimentation is extremely small compared to the initial value of r_i. This implies that the effect of acceleration occurring in the very early period of sedimentation is negligibly small. It is also found that the slope of a straight line related to the settling rate is little influenced by the initial height of the sample, in accordance with Work–Kohler relation (Work and Kohler, 1940; Iritani *et al.*, 2007). **Figure 6** shows the normalized sedimentation curve with varying α_S and constant ϕ (=0.17) (Figure 6(a)), and with varying ϕ and constant α_S (=0.75) (Figure 6(b)). The settling rate decreases with increasing α_S due to the slower settling rate of small particles and decreases with increasing ϕ due to the increase in the hindering effect.

When the sedimentation coefficient S is constant during the course of centrifugal sedimentation, integrating r_i in Eq. (10) from r_0 to r_i, the term $(r_i - r_0)/(R - r_0)$ appearing in the normalized sedimentation curve can be described by

$$\frac{r_i - r_0}{R - r_0} = \frac{r_0}{R - r_0}\left(e^{\Omega^2 St} - 1\right) \tag{11}$$

The solid lines in Figures 5 and 6 are calculations obtained by substituting Eqs. (5) and (7) into Eq. (11), indicating the model well describes the centrifugal sedimentation behaviors of bidisperse suspension in the initial period of sedimentation. The calculations can be approximated by the

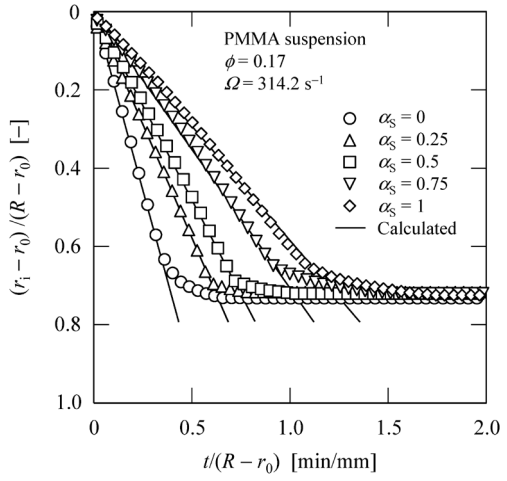

(a) Effect of ratio of volume of small to volume of total particles

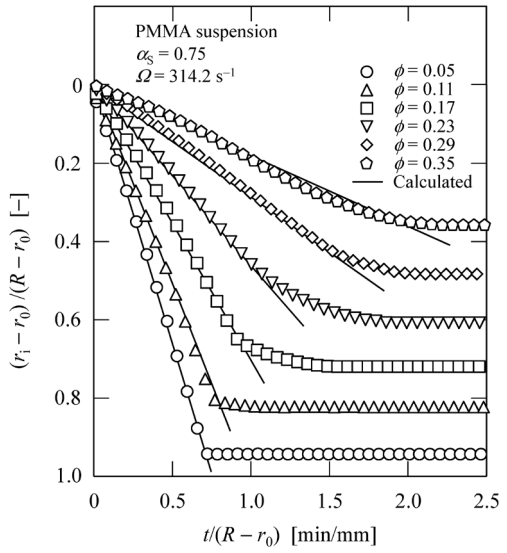

(b) Effect of volume fraction of total particles

Fig. 6 Normalized sedimentation curves under various conditions

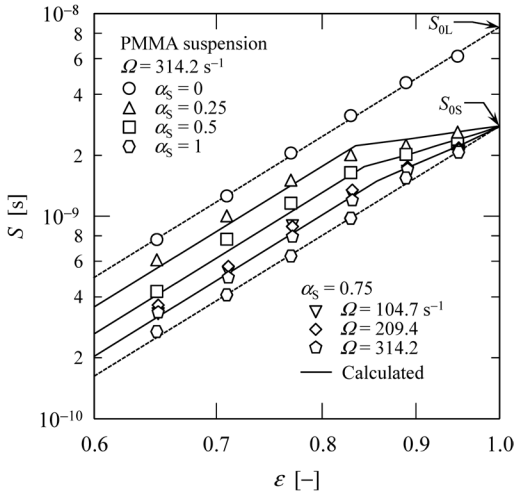

Fig. 7 Relation between sedimentation coefficient and porosity of suspension for several ratios of volume of small to volume of total particles

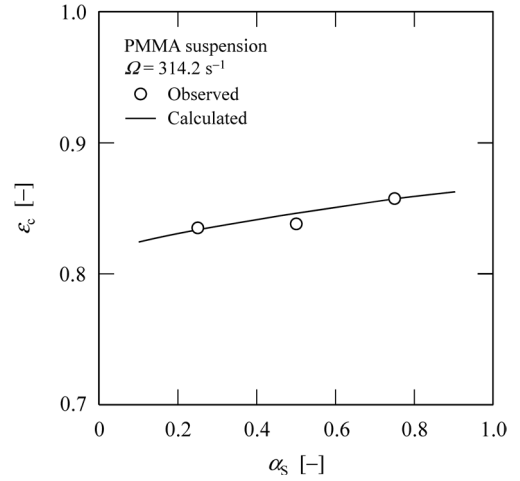

Fig. 8 Relation between critical porosity and ratio of volume of small to volume of total particles

straight lines throughout the initial period of sedimentation because the variation of centrifugal acceleration $r_i\Omega^2$ is negligible due to the slight change in r_i.

3.3 Dependence of sedimentation coefficient on porosity

In **Figure 7**, the sedimentation coefficient S obtained from centrifugal sedimentation is logarithmically plotted against the porosity ε on the total solid basis for various α_S values. The sedimentation coefficient S decreases with decreasing porosity ε and with increasing α_S. For monodisperse suspension ($\alpha_S = 0$, 1), each plot can be matched with Eq. (2) by inputting 5.56 as n. Thus, the intercepts of the lines on the ordinate axis at ε of 1.0 would give the Stokes sedimentation coefficients, S_{0S} and S_{0L}, of small and large particles in free settling. As a corollary, the Stokes diameters d_S and d_L are determined as 0.44, 0.77 μm, respectively. For a bidisperse suspension ($\alpha_S = 0.25$, 0.5, 0.75), the experimental data are in satisfactory agreement with the solid lines calculated from Eqs. (5) and (7). It should be noted that the slopes of the straight lines are all the same ($n = 5.56$) below the critical porosity ε_c. However, the slopes become smaller than 5.56 when the porosity is higher than ε_c. In addition, it is clear that S is little influenced by the magnitude of centrifugal acceleration, as seen in the plots for α_S of 0.75 and different values of Ω.

It is possible to determine the critical porosity ε_c experimentally from the sedimentation data on the basis of the curve fitting due to two lines drawn in the low and high concentration ranges. **Figure 8** compares the experimental data of critical porosity ε_c with the predictions obtained directly from Eq. (9) for different values of α_S, with relatively good agreement being observed. The critical porosity ε_c calculated from the model gradually increases with the increase in α_S and ranges from 0.818 to 0.866.

In **Figure 9**, the data shown in Figure 7 are replotted in the form of S/d_{av}^2 vs. ε in order to elucidate the influence of

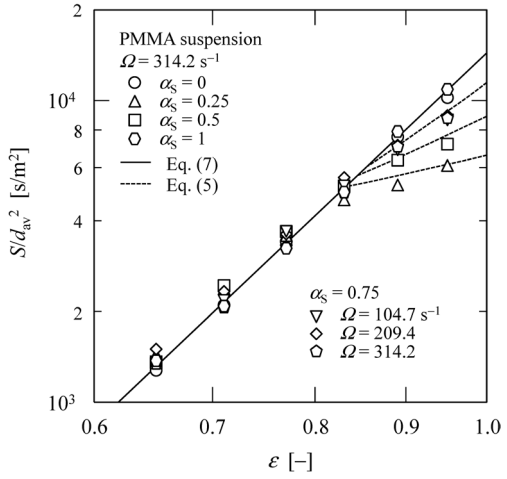

Fig. 9 Relation between sedimentation coefficient normalized by mean specific surface area size of particles and porosity in suspension

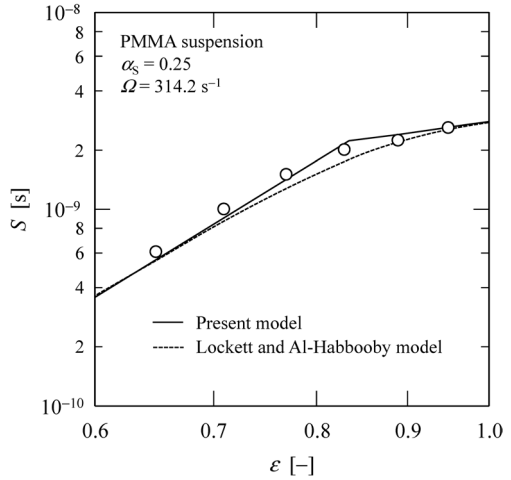

Fig. 10 Comparison of the present model calculations with Lockett and Al-Habbooby model calculations on relation between sedimentation coefficient and porosity of suspension

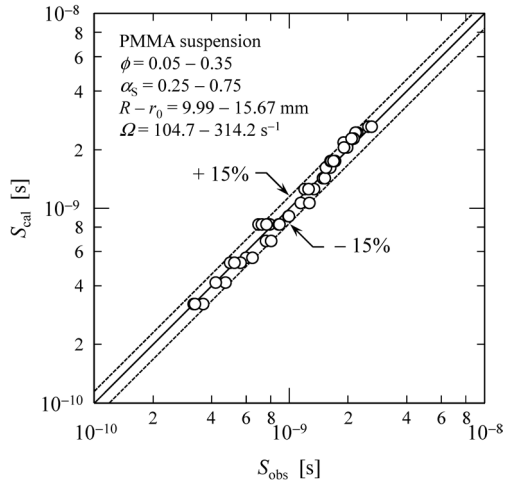

Fig. 11 Comparison of calculated values with experimental values on sedimentation coefficient

d_{av} in a mixed suspension on S. The solid line is the calculation obtained using Eq. (7) and is in fairly good agreement with the data for a monodisperse suspension and the data for a concentrated bidisperse suspension below the critical porosity ε_c. It should be noted that the calculations collapse to nearly a straight line irrespective of d_{av} when drawn in this manner. It must be stressed, once again, that the value of n is determined as 5.56, which is slightly smaller than the theoretical value of 6.55 indicated by Batchelor (1972). This difference arises probably because the van der Waals attractions between particles are not considered in Batchelor's theory (Al-Naafa and Selim, 1992). The data for a dilute bidisperse suspension above the critical porosity ε_c deviate from the solid straight line and shows smaller values since the small particles settling independently of large particles determines the settling rate of the solid–liquid interface in sedimentation. The dotted lines are the calculations obtained using Eq. (5) and roughly coincide with the data.

In **Figure 10**, S is plotted against ε for α_S of 0.25, and the present model calculations shown by the solid line are compared with Lockett and Al-Habbooby (1973) model calculations shown by the dotted line. It should be kept in mind that our model gives a slightly more satisfactory prediction of the experimental data compared with the Lockett and Al-Habbooby model despite the former being much more simplified than the latter. As mentioned in the foregoing, it is postulated in the Lockett and Al-Habbooby model that small particles settle separately from large particles.

In **Figure 11**, the calculations S_{cal} of the sedimentation coefficient are compared with the experimental values S_{obs} for a variety of values of ϕ, α_S, $(R-r_0)$, and Ω in the centrifugal sedimentation of a PMMA bidisperse suspension. All of the present data fall within the range bounded by the error bars of $\pm 15\%$ depicted by the dotted lines, indicating that the model can well describe the settling rate of the solid–liquid interface during the initial stage of the centrifugal sedimentation of a PMMA bidisperse suspension.

Conclusion

Centrifugal sedimentation experiments of concentrated bidisperse suspensions of spherical PMMA particles of two different sizes and equal densities in the submicron-sized range were conducted with the use of an analytical photocentrifuge. The influence of the porosity in suspension on the sedimentation coefficient for describing the settling rate of the interface between the dispersion and clear liquid was examined for different values of the ratio of the volume of small particles to the volume of total particles, initial height of the suspension, and angular velocity of the rotor. The experimental results showed that the sedimentation coefficient decreased with decreasing porosity and increasing ratio of the volume of small particles to volume of total particles. A new model was developed for describing the relation between the sedimentation coefficient and porosity in suspension in the centrifugal sedimentation of a bidisperse

suspension with the aid of the concept of critical porosity. The model developed here enabled us to readily evaluate the settling velocity of the interface between the dispersion and clear liquid in the centrifugal sedimentation of a bidisperse suspension from the centrifugal sedimentation data alone of each monodisperse suspension. Predictions from the model were in reasonable agreement with the experimental data acquired for a wide range of concentrations in colloids. The detailed dependence of the critical porosity on the size, size ratio, shape, etc. of small and large particles remains to be clarified.

Acknowledgements

This work has been partially supported by Grants-in-Aid for Scientific Research from the Ministry of Education, Culture, Sports, Science and Technology, Japan, from The Ministry of the Environment Goverment of Japan. The authors wish to acknowledge the financial support leading to the publication of this article with sincere gratitude. Da-Qi Cao also acknowledges funding from the China State-Sponsored "Postgraduate Study Abroad Program."

Nomenclature

C	=	constant defined by Eq. (4)	[s/m^2]
d	=	Stokes diameter of particles	[m]
d_{av}	=	mean specific surface area size of small and large particles	[m]
d_L	=	Stokes diameter of large particles	[m]
d_S	=	Stokes diameter of small particles	[m]
g	=	gravitational acceleration	[m/s^2]
n	=	empirical coefficient defined in Eq. (2)	[—]
R	=	radial distance from center of rotation to cell bottom	[m]
r	=	radial distance of arbitrary position from center of rotation	[m]
r_i	=	radial distance from center of rotation to interface of dispersion and clear liquid	[m]
r_0	=	radial distance from center of rotation to interface between dispersion filled in cell and air	[m]
S	=	sedimentation coefficient defined by Eq. (1)	[s]
S_0	=	sedimentation coefficient in free settling, calculated from Eq. (3)	[s]
S_{0S}	=	Stokes sedimentation coefficient of small particles in free settling	[s]
S_{0L}	=	Stokes sedimentation coefficient of large particles in free settling	[s]
T	=	NIR light transmission	[—]
t	=	centrifugal time	[s]
v	=	centrifugal settling velocity	[m/s]
α_S	=	ratio of volume of small to volume of total particles	[—]
ε	=	porosity defined as volume fraction of continuous phase	[—]
ε_S	=	porosity on small particle basis	[—]
ε_c	=	critical porosity in Eq. (9)	[—]
μ	=	viscosity of solvent	[Pa·s]
ρ	=	density of solvent	[kg/m^3]
ρ_P	=	density of particles	[kg/m^3]
ϕ	=	volume fraction of total particles	[—]
Ω	=	angular velocity of rotor	[s^{-1}]

‹Subscript›

cal	=	calculated value
obs	=	observed value

Literature Cited

Al-Naafa, M. A. and M. S. Selim; "Sedimentation of Monodisperse and Bidisperse Hard-Sphere Colloidal Suspensions," *AIChE J.*, **38**, 1618–1630 (1992)

Batchelor, G. K.; "Sedimentation in a Dilute Dispersion of Spheres," *J. Fluid Mech.*, **52**, 245–268 (1972)

Cao, D. Q., E. Iritani and N. Katagiri; "Flotation and Sedimentation Properties in Centrifugal Separation of Emulsion-Slurry," *J. Chem. Eng. Japan*, **47**, 392–398 (2014)

Cheung, M. K., R. L. Powell and M. J. McCarthy; "Sedimentation of Noncolloidal Bidisperse Suspensions," *AIChE J.*, **42**, 271–276 (1996)

Coulson, J. M., J. F. Richardson, J. R. Backhurst and J. H. Harker; "Sedimentation," Chemical Engineering, Vol. 2: Unit Operations, 3rd ed., p. 174, Pergamon Press, Oxford, U.K. (1978)

Davies, R.; "The Experimental Study of the Differential Settling of Particles in Suspension at High Concentrations," *Powder Technol.*, **2**, 43–51 (1968)

Detloff, T., T. Sobisch and D. Lerche; "Particle Size Distribution by Space or Time Dependent Extinction Profiles Obtained by Analytical Centrifugation," *Part. Part. Syst. Charact.*, **23**, 184–187 (2006)

Dorrell, R. and A. J. Hogg; "Sedimentation of Bidisperse Suspensions," *Int. J. Multiph. Flow*, **36**, 481–490 (2010)

Francis, A. W.; "Wall Effect in Falling Ball Method for Viscosity," *Physics*, **4**, 403–406 (1933)

Ha, Z. and S. Liu; "Settling Velocities of Polydisperse Concentrated Suspensions," *Can. J. Chem. Eng.*, **80**, 783–790 (2002)

Heitkam, S., Y. Yoshitake, F. Toquet, D. Langevin and A. Salonen; "Speeding Up of Sedimentation under Confinement," *Phys. Rev. Lett.*, **110**, 178302 (2013)

Hoyos, M., J. C. Bacri, J. Martin and D. Salin; "A Study of the Sedimentation of Noncolloidal Bidisperse, Concentrated Suspensions by an Acoustic Technique," *Phys. Fluids*, **6**, 3809–3817 (1994)

Iritani, E., K. Hattori and T. Murase; "Analysis of Dead-End Ultrafiltration Based on Ultracentrifugation Method," *J. Membr. Sci.*, **81**, 1–13 (1993)

Iritani, E., S. Akatsuka and T. Murase; "Sedimentation Behavior of Binary Protein Mixtures in Ultracentrifugation Field," *Kagaku Kogaku Ronbunshu*, **23**, 224–229 (1997)

Iritani, E., N. Katagiri, K. Aoki, M. Shimamoto and K. M. Yoo; "Determination of Permeability Characteristics from Centrifugal Flotation Velocity of Deformable Oil Droplets in O/W Emulsions," *Separ. Purif. Tech.*, **58**, 247–255 (2007)

Kondrat'ev, A. S. and E. A. Naumova; "Hindered Settling Velocity of a Bimodal Mixture of Spherical Solid Particles in a Newtonian Fluid," *Theor. Found. Chem. Eng.*, **40**, 387–392 (2006)

Krishnamoorthy, P., I. Reghupathi and T. Murugesan; "An Experimental Study and Correlation for Differential Settling of Bidisperse Suspensions," *Chem. Biochem. Eng. Q.*, **21**, 241–250 (2007)

Krishnamoorthy, P.; "Sedimentation Model and Analysis for Differential Settling of Two-Particle-Size Suspensions in the Stokes Region," *Int. J. Sediment Res.*, **25**, 119–133 (2010)

Lerche, D.; "Dispersion Stability and Particle Characterization by Sedimentation Kinetics in a Centrifugal Field," *J. Dispersion Sci. Technol.*, **23**, 699–709 (2002)

Lockett, M. J. and H. M. Al-Habbooby; "Differential Settling by Size of Two Particles Species in a Liquid," *Chem. Eng. Res. Des.*, **51**,

281–292 (1973)
Lockett, M. J. and H. M. Al-Habbooby; "Relative Particle Velocities in Two-Species Settling," *Powder Technol.*, **10**, 67–71 (1974)
Loginov, M., M. Citeau, N. Lebovka and E. Vorobiev; "Evaluation of Low-Pressure Compressibility and Permeability of Bentonite Sediment from Centrifugal Consolidation Data," *Separ. Purif. Tech.*, **92**, 168–173 (2012)
Mirza, S. and J. F. Richardson; "Sedimentation of Suspensions of Particles of Two or More Sizes," *Chem. Eng. Sci.*, **34**, 447–454 (1979)
Moore, W. J.; Physical Chemistry, 4th ed., pp. 938–939, Prentice-Hall, Inc., Upper Saddle River, U.S.A. (1972)
Richardson, J. F. and W. N. Zaki; "Sedimentation and Fluidisation: Part I," *Trans. IChemE*, **32**, 35–53 (1954)
Richardson, J. F. and R. A. Meikle; "Sedimentation and Fluidisation. Part-III. The Sedimentation of Uniform Fine Particles and Two-Component Mixtures of Solids," *Trans. IChemE*, **39**, 348–356 (1961)
Selim, M. S., A. C. Kothari and R. M. Turian; "Sedimentation of Multisized Particles in Concentrated Suspensions," *AIChE J.*, **29**, 1029–1038 (1983)
Smith, T. N.; "The Differential Sedimentation of Particles of Two Different Species," *Trans. Inst. Chem. Eng.*, **43**, T69–T73 (1965)
Smith, T. N.; "Differential Settling of a Binary Mixture," *Powder Technol.*, **92**, 171–178 (1997)
Work, L. T. and A. S. Kohler; "Sedimentation of Suspensions," *Ind. Eng. Chem.*, **32**, 1329–1334 (1940)
Yoshioka, N.; "Thickening (in Japanese)," Detailed Chemical Engineering: Unit Operations I (Shoron Kagaku Kogaku: Tan-i Sosa I), Y. Mori and F. Yoshida eds., p. 338, Asakura Shoten, Tokyo, Japan (1962)